



Article

Numerical Solution of Time Fractional Black–Scholes Model Based on Legendre Wavelet Neural Network with Extreme Learning Machine

Xiaoning Zhang [†] , Jianhui Yang ^{*} and Yuxin Zhao [†]

School of Business Administration, South China University of Technology, Guangzhou 510641, China; bmxnzhang@mail.scut.edu.cn (X.Z.); bmyxzhao@mail.scut.edu.cn (Y.Z.)

^{*} Correspondence: bmjhyang@scut.edu.cn; Tel.: +86-186-6609-2759

[†] These authors contributed equally to this work.

Abstract: In this paper, the Legendre wavelet neural network with extreme learning machine is proposed for the numerical solution of the time fractional Black–Scholes model. In this way, the operational matrix of the fractional derivative based on the two-dimensional Legendre wavelet is derived and employed to solve the European options pricing problem. This scheme converts this problem into the calculation of a set of algebraic equations. The Legendre wavelet neural network is constructed; meanwhile, the extreme learning machine algorithm is adopted to speed up the learning rate and avoid the over-fitting problem. In order to evaluate the performance of this scheme, a comparative study with the implicit differential method is constructed to validate its feasibility and effectiveness. Experimental results illustrate that this scheme offers a satisfactory numerical solution compared to the benchmark method.

Keywords: Legendre wavelet neural network (LWNN); operational matrix; extreme learning machine (ELM); Black–Scholes model; Caputo’s fractional derivative



Citation: Zhang, X.; Yang, J.; Zhao, Y.

Numerical Solution of Time

Fractional Black–Scholes Model

Based on Legendre Wavelet Neural

Network with Extreme Learning

Machine. *Fractal Fract.* **2022**, *6*, 401.

<https://doi.org/10.3390/fractalfract6070401>

Academic Editor: Ivanka Stamova

Received: 7 June 2022

Accepted: 15 July 2022

Published: 21 July 2022

Publisher’s Note: MDPI stays neutral with regard to jurisdictional claims in published maps and institutional affiliations.



Copyright: © 2022 by the authors. Licensee MDPI, Basel, Switzerland. This article is an open access article distributed under the terms and conditions of the Creative Commons Attribution (CC BY) license (<https://creativecommons.org/licenses/by/4.0/>).

1. Introduction

The options pricing model plays an important role in modern financial theory, which has been employed in cost budgets [1–3], asset valuations [4], resource allocation [5,6], and so on. It is of great significance to study options pricing and its modeling problem. The mathematical study of the financial market dates back to 1900 [7]. In 1973, the classic Black–Scholes model was proposed by Black and Scholes [8,9], which serves as a milestone of fair market options pricing. Over several decades, the B-S model has been extensively accepted because it can effectively model the options price and provides a mechanism for extracting implied volatility. Although the options price obtained from the B-S model can be well approximated to the observed one, it still has some deficiencies such as the failure to capture jump-diffusion over a small time frame in the financial market [10].

Being a generalization and extension of classic calculus, fractional calculus dates back to a letter from Leibniz to l’Hôpital in 1665 [11]. However, the theory and foundation of fractional calculus were developed by Liouville in 1832. After several decades, Grunwald and Letnikov defined the fractional derivative with differential quotient approach based on a fractional binomial expansion proposed by Newton. In 1967, Caputo defined Caputo’s fractional derivative, which requires the function to be differentiable [12]. In 2006, Jumarie made some improvements to the Riemann–Liouville derivative by subtracting a constant from the integrand to avoid the derivative of the constant being nonzero [13]. Guariglia and Silvestrov introduced the Ortigueira–Caputo fractional derivative operator to describe a complex function in the distribution sense [14]. Indeed, since some remarkable work appearing in [15], fractional calculus has become the key invariant, providing rich information about the level of complexity that a certain system presents. With plenty of research focusing on the fractional calculus field, it becomes imperative and necessary to solve the

fractional differential equation. An implicit method was proposed by Murio to solve the linear time fractional diffusion equation, constructed by Caputo's fractional derivative on a finite slab [16]. Langlands offered the stability and accuracy of the implicit numerical method for solving the fractional diffusion equation [17]. Chen proposed an explicit closed-form solution of the double-barrier option based on the time fractional B-S model [18], where the solution is obtained by the convolution of some specific function (Mittag-Leffler function) and finite series expansion with integration. As a consequence, some numerical methods were introduced to simplify the calculation procedure. Song adopted the implicit finite difference method to solve the options pricing problem based on Jumaire's model [19]. Cen [20] transformed the differential equation to an integral form with a weakly singular kernel and discretized it on an adaptive mesh grid, rigorously analyzed the convergence of the proposed scheme, and took account of possible singular behavior. Rezaei [21] presented the time fractional B-S model under the European double barrier option with the constant of elasticity of variance and presented the rigorous solvability, stability, and convergence of the implicit difference method. Zhang deduced an implicit discrete solution to the time fractional B-S model for the European option with double barriers, which has a spatially second-order accuracy and temporally $2 - \alpha$ -order accuracy [22]. De Staelen improved the spatial accuracy of the implicit differential method to fourth-order and presented the solvability, stability, and convergence of this method based on the Fourier method [23]. Moreover, some analytical methods have been derived, such as homotopy perturbation and the Laplace transform [24], the homotopy analysis method [25–30], the fractional variational iteration method [31,32], the generalized differential transform method [33], and the Adomian decomposition method [34–37]. The essential aspects of these methods are the convolution of some special function or the integration of infinite series expansion, which are complicated to calculate; what is more, the solvability, stability, and convergence need to be proven. As a consequence, making some improvements to the numerical method becomes practical and necessary.

Compared with standard Brownian motion, fractional Brownian motion can describe the dynamic characteristics of financial markets accurately; meanwhile, some new fractional B-S formulae have been derived. The fractional B-S model for the European option was initially proposed by Wyss [38], then Hu and Oksendal derived a fractional B-S model based on fractional Brownian motion [39]. Li developed a fractional stochastic differential equation to demonstrate the existence of trend memory in options pricing when the Hurst index is between 0.5 and 1 [40]. Jumarie proposed two new families of the fractional B-S model based on fractional Taylor expansion series and the modified Riemann–Liouville derivative [41]. Liu and Chang also proposed a time fractional B-S model with transaction cost based on fractional Brownian motion and provided an approximate solution of the nonlinear Hoggard–Whalley–Wilmott equation [42].

Accompanying the evolution of computer technology, machine learning has gained enormous advancement. Being a branch of artificial intelligence, reliable decisions and results can be obtained through iteration and optimization. In the last decade, a single feed-forward neural network named extreme learning machine [43,44] was proposed by Huang, which is different from traditional learning methods based on the gradient descent principle; meanwhile, the single hidden layer structure makes its learning procedure exceptionally faster compared with that of a deep neural network [45,46]; however, the ELM algorithm has been demonstrated to be sensitive to the activation function [47–49]. Furthermore, the wavelet can be regarded as a mathematical microscope for signal analysis (constant ratio of bandwidth and central frequency); its multi-resolution analysis and time–frequency ability can provide a powerful tool for signal analysis and approximation, then different wavelets can be constructed by dilation and translation, such as the Legendre wavelet [50], Chebyshev wavelet [51], Taylor wavelet [52], etc. Aiming at the framework of an adaptive multi-scale wavelet, Zheng pointed out that a sampling rate far from 1/2 can lead to low representation efficiency and proposed a signal Shannon-entropy-based adaptive multi-scale wavelet decomposition for signals analysis [53]. The wavelet neural network, suggested by Zhang in 1992 [54], was initially used for signal approximation [55], which

can be applied in image analysis and computer vision, such as video segmentation [56], speech recognition, and data compression [57]. Besides, some improved neural-network-based methods have recently emerged; however, these methods lack a strong theoretical foundation and require massive amounts of training data. Shi et al. proposed the deep scattering network (DSN), a variant of the deep convolutional neural network (DCNN), where the data-driven linear filters are replaced by predefined fixed multi-scale wavelet filters; for the non-stationary image textures, the fractional wavelet transform (FRWT) is employed because it can be regarded as a bank of linear translation-variant multi-scale filters [58]. Aiming at poor resolution in the high-fractional-frequency domain, Shi and his partners revealed a novel fractional wavelet package transform (FRWPT) and its recursive algorithm [59].

Moreover, previous literature demonstrated the reliability and stability of the WNN in the learning procedure [60,61]. Due to the decomposition capacity of the WNN in the time and frequency domain, this paper presents a novel Legendre wavelet neural network (LWNN) with extreme learning machine (ELM) to solve the time fractional B-S model governed by the European option. Taking the final and boundary conditions into consideration, this time fractional B-S model can be converted into a group of algebraic equations. In the end, numerical experiments illustrate the superiority of the proposed method compared to the implicit differential method.

The objective of this paper is to solve a time fractional B-S model of the European option, where ELM is used for the output layer weight learning of the LWNN. The advantages of the proposed scheme are given as follows:

- It is a single hidden layer feed-forward network; we only should train the weights of the output layer; the input layer weights can be randomly selected.
- ELM can be classified as unsupervised learning; the optimization scheme is unnecessary; besides, it has a fast learning rate and can avoid over-fitting.
- It converts the European options pricing problem to a group of algebraic equations, which can substantially facilitate analysis.

The structure of this paper is as follows. Section 2 gives a description of the time fractional B-S model governed by the European option with double barriers. Section 3 introduces the properties of the Legendre wavelet. Section 4 deduces the operational matrix of the fractional derivative for the two-dimensional Legendre wavelet. Section 5 presents the topology of the LWNN and the algorithm of ELM. Section 6 validates the feasibility and effectiveness of the proposed method by numerical experiments. In the end, some conclusions and directions for improvement are presented.

2. Double Barrier Option under Time Fractional B-S Model

2.1. Time Fractional B-S Model

Liang [62] proposed a bi-fractional B-S model in the time and spatial domain, where the underlying asset price follows a fractional Ito process and options price variation is a fractal transmission system. As a result, the time fractional B-S model can be regarded as a special case of the bi-fractional B-S model. Let S , t , r , σ , and q be the underlying asset price, time, risk-free interest rate, volatility, and dividend payment, respectively, then options price $V(S, t)$ should satisfy

$$\frac{\partial V}{\partial t} + \frac{1}{2}\sigma^2 S^2 \frac{\partial^2 V}{\partial S^2} + (r - q)S \frac{\partial V}{\partial S} - rV = 0 \quad (1)$$

According to the arguments in [62–64], the variation of the options price regarding time can be assumed as a fractal transmission system, which implies that the average options price $C(S, t)$ from time t to expiration time T should satisfy

$$\int_t^T C(S, \tau) d\tau = S^{d_f-1} \int_t^T F(\tau - t) [V(S, \tau) - V(S, T)] d\tau \quad (2)$$

where $F(t)$ and d_f represent the transmission function and Hausdorff dimension of the fractional transmission system, respectively. As pointed out in [62], Equation (2) is a conservation equation containing an explicit reference to the diffusion process of the options price based on a fractal structure. It can be assumed that the diffusion sets are the underlying fractal, where $F(t) = A_\alpha t^{-\alpha} / \Gamma(1 - \alpha)$ is selected as the transmission function with A_α and α a constant and the transmission exponent, respectively. Making partial differentiation regarding t on both sides of Equation (2) yields

$$-C(S, t) = S^{d_f-1} \frac{\partial}{\partial t} \int_t^T F(\tau - t) [V(S, \tau) - V(S, T)] d\tau \quad (3)$$

On the other hand, because of the B-S model, we have

$$C(S, t) = \frac{1}{2} \sigma^2 S^2 \frac{\partial^2 V}{\partial S^2} + (r - q) S \frac{\partial V}{\partial S} - rV \quad (4)$$

substituting Equation (3) into (4) yields

$$A_\alpha S^{d_f-1} \frac{\partial^\alpha V}{\partial t^\alpha} + \frac{1}{2} \sigma^2 S^2 \frac{\partial^2 V}{\partial S^2} + (r - q) S \frac{\partial V}{\partial S} - rV = 0 \quad (5)$$

where

$$\frac{\partial^\alpha V}{\partial t^\alpha} = \frac{1}{\Gamma(n - \alpha)} \frac{\partial^n}{\partial t^n} \int_t^T \frac{V(S, \tau) - V(S, T)}{(\tau - t)^{\alpha+1-n}} d\tau, \quad n - 1 \leq \alpha < n \quad (6)$$

when α approaches 1, this yields

$$\lim_{\alpha \rightarrow 1} \frac{\partial^\alpha V}{\partial t^\alpha} = \frac{1}{\Gamma(2 - 1)} \frac{\partial}{\partial t} \int_t^T \frac{V(S, \tau) - V(S, T)}{(\tau - t)^{1+1-2}} d\tau = \frac{\partial V}{\partial t}$$

It is clear that the time fractional B-S model is consistent with the classic B-S model when $A_\alpha = d_f = 1$. In this paper, $A_\alpha = d_f = 1$ are selected. As a matter of fact, the solution procedure is applicable to other values of A_α and d_f .

It should be mentioned that the time fractional order model is a simplification compared with that proposed by Liang [62]. In this paper, we assume that the underlying asset follows standard Brownian motion, only considering the options price variation with time as a fractal transmission system; this is why the fractional derivative only appears in the time domain. Actually, Jumaire [65,66] defined the stock exchange fractional dynamics as fractional exponential growth driven by Gaussian noise; it can be found that the derived equation is similar to Equation (5). However, the derived equation has a time variable coefficient in front of the second derivative, which is different from the time fractional B-S model mentioned above.

2.2. Double Barrier Option

The barrier option is probably the oldest exotic option, which was sporadically traded on the U.S. market before the establishment of the Chicago Board of Options Exchange. The barrier option is essentially a conditional option, depending on whether the barrier can be triggered or breached within its expiration; meanwhile, it is considerably less expensive than the corresponding vanilla option. Obviously, a double barrier option features two barriers, and the payoff to the holder depends on the breaching behaviors of the underlying asset process with respect to these two barriers. Let $V(S, t)$ be the price of a European option with double barriers; obviously, if the price variation regarding time is considered to be a fractal transmission system, then $V(S, t)$ should satisfy

$$\begin{cases} \frac{\partial^\alpha V}{\partial t^\alpha} + \frac{1}{2}\sigma^2 S^2 \frac{\partial^2 V}{\partial S^2} + (r - q)S \frac{\partial V}{\partial S} - rV = 0 \\ V(S, T) = \overline{P}(S) = \max(S - k, 0) \\ V(A, t) = \overline{P}(t) \\ V(B, t) = \overline{Q}(t) \end{cases} \quad (7)$$

where $\overline{P}(t)$ and $\overline{Q}(t)$ denote the discount paid when the corresponding barrier is breached and K and T are the strike price and expiration time, respectively. In general, it is complicated to obtain the solution of this partial derivative equation; the following variables and functions are introduced to non-dimensionalize this model: $t = T - 2\tau/(\sigma^2)$, $S = Ke^x$, $V(S, t) = KU(x, \tau)$, $\overline{P}(t) = KP(\tau)$, and $\overline{Q}(t) = KQ(\tau)$; as a consequence, the European Equation (7) can be rewritten as

$$\begin{aligned} \frac{\partial^\alpha V}{\partial t^\alpha} &= \frac{1}{\Gamma(1-\alpha)} \frac{\partial}{\partial t} \int_t^T \frac{V(S, \bar{t}) - V(S, T)}{(\bar{t} - t)^\alpha} d\bar{t} \\ &= \frac{1}{\Gamma(1-\alpha)} \left(-\frac{\sigma^2}{2}\right) \frac{\partial}{\partial \tau} \int_{T-\frac{2\tau}{\sigma^2}}^T \frac{V(S, \bar{t}) - V(S, T)}{\left[\bar{t} - \left(T - \frac{2\tau}{\sigma^2}\right)\right]^\alpha} d\bar{t} \\ &= \frac{1}{\Gamma(1-\alpha)} \left(-\frac{\sigma^2}{2}\right) \frac{\partial}{\partial \tau} \int_\tau^0 \frac{V\left(S, T - \frac{2\bar{\tau}}{\sigma^2}\right) - V(S, T)}{\left[\frac{2}{\sigma^2}(\tau - \bar{\tau})\right]^\alpha} \left(-\frac{2}{\sigma^2}\right) d\bar{\tau} \\ &= \frac{-K}{\Gamma(1-\alpha)} \left(\frac{\sigma^2}{2}\right)^\alpha \frac{\partial}{\partial \tau} \int_0^\tau \frac{U(x, \bar{\tau}) - U(x, 0)}{(\tau - \bar{\tau})^\alpha} d\bar{\tau} = -K \left(\frac{\sigma^2}{2}\right)^\alpha \frac{\partial^\alpha U}{\partial \tau^\alpha} \end{aligned} \quad (8)$$

where

$$\frac{\partial^\alpha U}{\partial t^\alpha} = \frac{1}{\Gamma(1-\alpha)} \frac{\partial}{\partial t} \int_0^t \frac{U(x, \tau) - U(x, 0)}{(\tau - t)^\alpha} d\tau, \quad 0 < \alpha < 1$$

is consistent with the modified Riemann–Liouville derivative in [13]. Substituting Equation (8) into Equation (7) yields

$$\begin{cases} \frac{\partial^\alpha U}{\partial \tau^\alpha} = c_1 \frac{\partial^2 U}{\partial x^2} + c_2 \frac{\partial U}{\partial x} + c_3 U \\ U(x, 0) = \Pi(x) \\ U(B_d, \tau) = P(\tau) \\ U(B_u, \tau) = Q(\tau) \end{cases} \quad (9)$$

where $\gamma = r(-\sigma^2/2)^{-\alpha}$, $d = q(\sigma^2/2)^{-\alpha}$, $c_1 = (\sigma^2/2)^{1-\alpha}$, $c_2 = r - d - c_1$, $c_3 = -\gamma$, $B_d = \ln(A/K)$, and $B_u = \ln(B/K)$. It can be observed that $\frac{\partial^\alpha U}{\partial \tau^\alpha}$ is consistent with Caputo's derivative in Definition 2.

3. Legendre Wavelet and Its Properties

Legendre polynomials are constructed by the polynomials', $\{1, x, \dots, x^n, \dots\}$, orthogonalization with respect to weighting function $w(x) = 1$. In 1814, Rodrigul presented the simple expression as

$$L_0(x) = 1, \quad L_n(x) = \frac{1}{2^n n!} \frac{d^n}{dx^n} \{(x^2 - 1)^n\}, \quad x \in [-1, 1], \quad n \in \mathbb{Z}^+ \quad (10)$$

In [67], the recurrence formula of Legendre polynomials was given as

$$\begin{cases} L_0(x) = 1, \quad L_1(x) = x \\ L_{n+1}(x) = \frac{2n+1}{n+1} x L_n(x) - \frac{n}{n+1} L_{n-1}(x) \end{cases} \quad (11)$$

For the practical implementation of Legendre polynomials on domain $[l_d, l_u]$, it is feasible to shift the domain by means of linear transformation $\tilde{x} = [2x - (l_u + l_d)] / (l_u - l_d)$. Hence, the shifted Legendre polynomials $L_n^*(x)$ can be obtained as $L_n^*(x) = L_n(\tilde{x})$. Specifically, the orthogonality characteristic of shifted Legendre polynomials on domain $[0, 1]$ is

$$\int_0^1 L_m^*(x) L_n^*(x) dx = \begin{cases} \frac{1}{2m+1}, & m = n \\ 0, & \text{otherwise} \end{cases} \quad (12)$$

Moreover, the analytical form of shifted Legendre polynomials $L_n^*(x)$ can be expressed as [67]

$$L_n^*(x) = \sum_{i=0}^n b_{n,i} x^i \quad (13)$$

where

$$b_{n,i} = (-1)^{n+i} \frac{(n+i)!}{(n-i)!(i!)^2}$$

Furthermore, the wavelet function is generally constructed by the dilation and translation of the mother wavelet. When the dilation and translation parameters vary continuously, we can obtain the continuous wavelet:

$$\psi_{a,b}(x) = \frac{1}{\sqrt{a}} \psi\left(\frac{x-b}{a}\right), \quad a, b \in \mathbb{R}, \quad a > 0 \quad (14)$$

where a and b are the dilation and translation parameters, respectively. When they are constricted to only discrete values $a = a_0^k, b = na_0^k b_0, a_0 > 1, b_0 > 1$, this yields

$$\psi_{k,n}(x) = \frac{1}{\sqrt{a_0^k}} \psi\left(\frac{x - na_0^k b_0}{a_0^k}\right) = a_0^{-k/2} \psi(a_0^{-k} x - nb_0), \quad n, k \in \mathbb{Z}^+ \quad (15)$$

where $\psi_{k,n}(x)$ represents the basis of $L^2(R)$. In particular, $\psi_{k,n}(x)$ constructs an orthogonal basis when $a_0 = 2$ and $b_0 = 1$. Legendre wavelet $\psi_{n,m}(t) = \psi(k, \hat{n}, m, t)$ is composed of four arguments, $\hat{n} = 2n + 1, n = 0, 1, 2, \dots, 2^{k-1}, m = 0, 1, \dots, m_0 - 1$ is the degree of the Legendre polynomials, and t is normalized time [68]. The Legendre wavelet on domain $[0, 1]$ is defined as

$$\psi_{n,m}(x) = \begin{cases} \sqrt{2m+1} \sqrt{2^k} L_m(2^{k+1}x - \hat{n}), & \frac{n}{2^k} \leq x \leq \frac{n+1}{2^k} \\ 0, & \text{otherwise} \end{cases} \quad (16)$$

Theorem 1. [[69]] Supposing that \mathcal{H} and $\mathcal{Y} \subset \mathcal{H}$ are the inner product and complete space, respectively, we define $\{e_0, e_1, \dots, e_n\}$ as an orthogonal basis for \mathcal{H} . For $f \in \mathcal{H}$, the best approximation in \mathcal{Y} :

$$f_0 = \sum_{i=0}^n (f, e_i) e_i$$

such that

$$\forall y \in \mathcal{Y}, \quad \|f - f_0\|_2 \leq \|f - y\|_2$$

where (\cdot) denotes the inner product, that is $\|f\|_2 = \sqrt{(f, f)}$.

From Theorem 1, a function $f(x)$ on domain $[0, 1]$ can be expanded by the Legendre wavelet as

$$f(x) = \sum_{n=0}^{\infty} \sum_{m=0}^{\infty} c_{n,m} \psi_{n,m}(x) \quad (17)$$

where $c_{n,m} = (f(x), \psi_{n,m}(x))$. If Equation (17) is substituted with finite series expansion, then $f(x)$ can be written as

$$f(x) \simeq \sum_{n=0}^{2^k-1} \sum_{m=0}^{m_0-1} c_{n,m} \psi_{n,m}(x) = C^T \Psi(x) \quad (18)$$

where T represents the matrix transposition operator and C and $\Psi(x)$ are the $2^k m_0$ -column vector shown as below.

$$C = [c_{0,0}, c_{0,1}, \dots, c_{0,m_0-1}, c_{1,0}, c_{1,1}, \dots, c_{1,m_0-1}, \dots, c_{2^k-1,0}, c_{2^k-1,1}, \dots, c_{2^k-1,m_0-1}]^T$$

$$\Psi(x) = [\psi_{0,0}(x), \psi_{0,1}(x), \dots, \psi_{0,m_0-1}(x), \psi_{1,0}(x), \psi_{1,1}(x), \dots, \psi_{1,m_0-1}(x), \dots, \psi_{2^k-1,0}(x), \psi_{2^k-1,1}(x), \dots, \psi_{2^k-1,m_0-1}(x)]^T$$

For simplicity, let $c_i = c_{n,m}$, $\psi_i = \psi_{n,m}$, and $M = 2^k m_0$, where index i is determined by $i = m_0 n + m + 1$, then Equation (18) can be rewritten as

$$f(x) \simeq \sum_{i=1}^M c_i \psi_i(x) = C^T \Psi(x) \quad (19)$$

where

$$C = [c_1, \dots, c_{m_0}, |, c_{m_0+1}, \dots, c_{2m_0}, |, c_{m_0(2^k-1)+1}, \dots, c_M]^T$$

$$\Psi(x) = [\psi_1(x), \dots, \psi_{m_0}(x), |, \psi_{m_0+1}(x), \dots, \psi_{2m_0}(x), |, \dots, |, \psi_{m_0(2^k-1)+1}(x), \dots, \psi_M(x)]^T$$

Similarly, an arbitrary function with two variables $f(x, y) \in \mathbb{L}^2(\mathbb{R} \times \mathbb{R})$ defined on domain $[0, 1] \times [0, 1]$ can be approximated with the Legendre wavelet:

$$f(x, y) \simeq \sum_{i=1}^M \sum_{j=1}^M \psi_i(x) f_{ij} \psi_j(y) = \Psi^T(x) F \Psi(y) \quad (20)$$

where $F = [f_{ij}]_{M \times M}$ and $f_{ij} = (\psi_i(x), (f(x, y), \psi_j(y)))$.

Theorem 2. [Convergence analysis [70]] *Supposing that a continuous function $f(x)$ on domain $[0, 1]$ is bounded with second derivative $|f''(x)| \leq K$, it can be uniformly approximated by the infinite sum of Legendre wavelet expansion, that is $f(x) = \sum_{n=1}^{\infty} \sum_{m=0}^{\infty} c_{n,m} \psi_{n,m}(x)$; moreover, coefficients $c_{n,m}$ are bounded with $|c_{n,m}| \leq K\sqrt{12}/(2n)^{5/2}(2m-3)^2$.*

Theorem 3. [Error analysis [71]] *Supposing that a continuous function $f(x, y)$ on domain $[0, 1] \times [0, 1]$ is bounded with four mixed partial derivatives $|\partial^4 f(x, y)/\partial x^2 \partial y^2| \leq D$, then the Legendre wavelet expansion of $f(x, y)$ has a uniform convergence characteristic and*

$$|f_{ij}| < \frac{12D}{(2n)^5(2m-3)^4}$$

Definition 1. Supposing that $A = [a_{ij}]_{m \times n}$ and $B = [b_{ij}]_{p \times q}$ are two arbitrary matrices, the Kronecker product of A and B is defined as follows [72].

$$A \otimes B = \begin{bmatrix} a_{11}B & a_{12}B & \cdots & a_{1n}B \\ a_{21}B & a_{22}B & \cdots & a_{2n}B \\ \vdots & \vdots & \ddots & \vdots \\ a_{m1}B & a_{m2}B & \cdots & a_{mn}B \end{bmatrix}_{mp \times nq}$$

For matrix A , operator $\text{Vec}(A)$ is a column vector made of the column of A stacked on top of each other from left to right [73].

$$\text{Vec}(A) = [a_{11}, \dots, a_{m1}, a_{12}, \dots, a_{m2}, \dots, a_{1n}, \dots, a_{mn}]^T$$

Definition 2. The Caputo's fractional derivative of order α is defined as [74]

$${}_0^C D_x^\alpha f(x, y) = \begin{cases} \frac{1}{\Gamma(n - \alpha)} \int_0^x \frac{f^{(n)}(\chi, y)}{(x - \chi)^{1 + \alpha - n}} d\chi, & 0 \leq n - 1 < \alpha < n \\ \frac{\partial^\alpha f(x, y)}{\partial x^\alpha}, & \alpha = n \end{cases}$$

where operator D_*^α represents Caputo's derivative. It can be observed that $D_x^\alpha C = 0$ (C is a constant); additionally,

$$D_x^\alpha x^n = \begin{cases} 0, & n < \lceil \alpha \rceil, n \in \mathbb{Z}^+ \\ \frac{\Gamma(n + 1)}{\Gamma(n + 1 - \alpha)} x^{n - \alpha}, & n \geq \lceil \alpha \rceil, n \in \mathbb{Z}^+ \end{cases}$$

where $\Gamma(\cdot)$ denotes the Gamma function; the ceiling function $\lceil \alpha \rceil$ denotes the smallest integer greater than or equal to α .

4. Operational Matrix of Fractional Derivative

From Equations (13) and (16), for $m < \lceil \alpha \rceil$, the analytical form of the shifted Legendre wavelet can be written as

$$\psi_{n,m}(x) = 2^{k/2} \sqrt{2m + 1} \sum_{i=0}^m b_{m,i} (2^k x - n)^i I_{n,k}(x) \quad (21)$$

where $I_{n,k} = \left[n/2^k, (n + 1)/2^k \right]$ ($n = 0, 1, \dots, 2^k - 1$, $m = 0, 1, \dots, m_0 - 1$); in addition, the indicator function is defined as

$$I_{n,k}(x) = \begin{cases} 1, & x \in \left[\frac{n}{2^k}, \frac{n + 1}{2^k} \right] \\ 0, & \text{otherwise} \end{cases}$$

It is apparent that $I_{n,k}(x)$ is zero outside the interval $\left[n/2^k, (n + 1)/2^k \right]$. Applying D_x^α on both sides of Equation (21) yields

$$\begin{aligned} D_x^\alpha \psi_{n,m}(x) &= \sum_{i=0}^m D^\alpha \left(\left(x - \frac{n}{2^k} \right)^i \right) = \sum_{i=\lceil \alpha \rceil}^m \frac{a_{m,i}(i)!}{\Gamma(i - \alpha + 1)} \left(x - \frac{n}{2^k} \right)^{i - \alpha} I_{n,k}(x) \\ &\quad + \sum_{i=\lceil \alpha \rceil}^m \frac{a_{m,i}(i)!}{\Gamma(\lceil \alpha \rceil - \alpha) \Gamma(i - \lceil \alpha \rceil + 1)} f_i(x) \end{aligned} \quad (22)$$

where

$$a_{m,i} = 2^{k(i+1/2)} \sqrt{2m+1} b_{m,i}, \quad f_i(x) = \int_{n/2^k}^{(n+1)/2^k} \frac{\left(x - \frac{n}{2^k}\right)^{i-\lceil\alpha\rceil}}{(x-\chi)^{\alpha-\lceil\alpha\rceil+1}} d\chi$$

Here, Legendre wavelet expansions are employed to approximate $(x - n/2^k)^{i-\alpha}$, that is to say

$$\left(x - \frac{n}{2^k}\right)^{i-\alpha} = \sum_{j=0}^{m_0-1} e_{i,j} \psi_{n,j}(x), \quad i = \lceil\alpha\rceil, \lceil\alpha\rceil + 1, \dots, m \quad (23)$$

where

$$\begin{aligned} e_{i,j} &= \int_{n/2^k}^{(n+1)/2^k} \left(x - \frac{n}{2^k}\right)^{i-\alpha} \psi_{n,j}(x) dx \\ &= \sum_{r=0}^j c_{j,r} \int_{n/2^k}^{(n+1)/2^k} (2^k x - n)^{r+i-\alpha} dx = \sum_{r=0}^j \frac{c_{j,r}}{2^k(r+i-\alpha+1)} \end{aligned}$$

and

$$c_{j,r} = \frac{2^{k/2} \sqrt{2m+1}}{2^{k(i-\alpha)}} b_{j,r}$$

Furthermore, $f_i(x)$ in Equation (22) can be approximated by the Legendre wavelet in every interval $I_{l,k}(x)$, $l = n+1, \dots, 2^k-1$, yielding

$$f_i(x) = \sum_{j=0}^{m_0-1} d_{i,j} \psi_{l,j}(x) \quad (24)$$

where

$$\begin{aligned} d_{i,j} &= \int_{l/2^k}^{(l+1)/2^k} f_i(x) \psi_{l,j}(x) dx \\ &= \sum_{r=0}^j 2^{k/2} \sqrt{2m+1} b_{j,r} \times \int_{l/2^k}^{(l+1)/2^k} f_i(x) (2^k x - l)^r dx \end{aligned}$$

Substituting Equations (23) and (24) into Equation (22), we can obtain

$$D_x^\alpha \psi_{n,m}(x) = \sum_{j=0}^{m_0-1} \Omega_\alpha^{(n)}(m, j) \psi_{n,j}(x) + \sum_{l=n+1}^{2^k-1} \sum_{j=0}^{m_0-1} \hat{\Omega}_\alpha^{(n)}(m, j) \psi_{l,j}(x) \quad (25)$$

where

$$\begin{cases} \Omega_\alpha^{(n)}(m, j) = \sum_{i=\lceil\alpha\rceil}^m \Theta_{m,j,i} \\ \Theta_{m,j,i} = \frac{a_{m,i}(i)!}{\Gamma(i-\alpha+1)} \times \sum_{r=0}^j \frac{c_{j,r}}{2^k(r+i-\alpha+1)} \end{cases}$$

and

$$\begin{cases} \hat{\Omega}_\alpha^{(n)}(m, j) = \sum_{i=\lceil \alpha \rceil}^m \hat{\Theta}_{m,j,i} \\ \hat{\Theta}_{m,j,i} = \frac{a_{m,i}(i)!}{\Gamma(\lceil \alpha \rceil - \alpha) \Gamma(i - \lceil \alpha \rceil + 1)} \times \sum_{r=0}^j 2^{k/2} \sqrt{2m+1} b_{j,r} \times \\ \int_{l/2^k}^{(l+1)/2^k} f_i(x) (2^k x - l)^r dx \end{cases}$$

After simplification, $\Theta_{m,j,i}$ and $\hat{\Theta}_{m,j,i}$ can be written as:

$$\Theta_{m,j,i} = \frac{(-1)^{m+i+j} 2^{k\alpha} (2m+1)(m+i)! \Gamma(i-\alpha+2) \Gamma(j-i+\alpha)}{(i-\alpha+1)(m-i)!(i)! \Gamma(-i+\alpha) \Gamma(i-\alpha+1) \Gamma(j+i-\alpha+2)} \quad (26)$$

and

$$\hat{\Theta}_{m,j,i} = \frac{2^{k(i+1)} (2m+1) b_{m,i}(i)!}{\Gamma(\lceil \alpha \rceil - \alpha) \Gamma(i - \lceil \alpha \rceil + 1)} \sum_{r=0}^j b_{j,r} \int_{l/2^k}^{(l+1)/2^k} f_i(x) (2^k x - l)^r dx \quad (27)$$

Consequently, Equation (25) can be written as

$$\begin{aligned} D_x^\alpha \psi_{n,m}(x) &= [\Omega_\alpha^{(n)}(m, 0), \Omega_\alpha^{(n)}(m, 1), \dots, \Omega_\alpha^{(n)}(m, m_0 - 1)] \Psi_n(x) + \\ &\sum_{l=n+1}^{2^k-1} [\hat{\Omega}_\alpha^{(n)}(m, 0), \hat{\Omega}_\alpha^{(n)}(m, 1), \dots, \hat{\Omega}_\alpha^{(n)}(m, m_0 - 1)] \Psi_l(x) \end{aligned} \quad (28)$$

where

$$\Psi_s(x) = [\psi_{s,0}(x), \psi_{s,1}(x), \dots, \psi_{s,(m_0-1)}(x)], \quad s = 0, 1, 2, \dots, 2^k - 1$$

Remark 1. For $\alpha = \lceil \alpha \rceil$, from Caputo's derivative, we can obtain

$$D_x^\alpha \psi_{n,m}(x) = \begin{cases} 0, & 0 \leq m < \lceil \alpha \rceil \\ \sum_{j=0}^{m_0-1} \Omega_\alpha^{(n)}(m, j) \psi_{n,j}(x), & m \geq \lceil \alpha \rceil \end{cases} \quad (29)$$

Let $\Psi(x)$ be the Legendre wavelet vector in Equation (18), D^α ($\alpha > 0$, and $(\lceil \alpha \rceil - 1 < \alpha < \lceil \alpha \rceil)$) be the α -order differential operational matrix of the Legendre wavelet, then

$$D_x^\alpha \Psi(x) \simeq D^\alpha \Psi(x) \quad (30)$$

where

$$D^\alpha = \begin{bmatrix} B^\alpha & F^\alpha & \dots & F^\alpha & F^\alpha \\ 0 & B^\alpha & \dots & F^\alpha & F^\alpha \\ \vdots & \vdots & \ddots & \vdots & \vdots \\ 0 & 0 & \dots & B^\alpha & F^\alpha \\ 0 & 0 & \dots & 0 & B^\alpha \end{bmatrix}_{M \times M}$$

where matrices B^α and F^α are given as

$$B^\alpha = \begin{bmatrix} 0 & 0 & \cdots & 0 \\ \vdots & \vdots & \cdots & \vdots \\ 0 & 0 & \cdots & 0 \\ \Omega_\alpha^{(n)}(\lceil \alpha \rceil, 0) & \Omega_\alpha^{(n)}(\lceil \alpha \rceil, 1) & \cdots & \Omega_\alpha^{(n)}(\lceil \alpha \rceil, m_0 - 1) \\ \Omega_\alpha^{(n)}(\lceil \alpha \rceil + 1, 0) & \Omega_\alpha^{(n)}(\lceil \alpha \rceil + 1, 1) & \cdots & \Omega_\alpha^{(n)}(\lceil \alpha \rceil + 1, m_0 - 1) \\ \vdots & \vdots & \cdots & \vdots \\ \Omega_\alpha^{(n)}(m_0 - 1, 0) & \Omega_\alpha^{(n)}(m_0 - 1, 1) & \cdots & \Omega_\alpha^{(n)}(m_0 - 1, m_0 - 1) \end{bmatrix}_{m_0 \times m_0}$$

and

$$F^\alpha = \begin{bmatrix} 0 & 0 & \cdots & 0 \\ \vdots & \vdots & \cdots & \vdots \\ 0 & 0 & \cdots & 0 \\ \hat{\Omega}_\alpha^{(n)}(\lceil \alpha \rceil, 0) & \hat{\Omega}_\alpha^{(n)}(\lceil \alpha \rceil, 1) & \cdots & \hat{\Omega}_\alpha^{(n)}(\lceil \alpha \rceil, m_0 - 1) \\ \hat{\Omega}_\alpha^{(n)}(\lceil \alpha \rceil + 1, 0) & \hat{\Omega}_\alpha^{(n)}(\lceil \alpha \rceil + 1, 1) & \cdots & \hat{\Omega}_\alpha^{(n)}(\lceil \alpha \rceil + 1, m_0 - 1) \\ \vdots & \vdots & \cdots & \vdots \\ \hat{\Omega}_\alpha^{(n)}(m_0 - 1, 0) & \hat{\Omega}_\alpha^{(n)}(m_0 - 1, 1) & \cdots & \hat{\Omega}_\alpha^{(n)}(m_0 - 1, m_0 - 1) \end{bmatrix}_{m_0 \times m_0}$$

Here, for a better understanding of the calculation procedure, $B^{(1.5)}$ and $F^{(1.5)}$ are provided as below, where $m_0 = 4$, $k = 2$, and $\alpha = 1.5$ are selected.

$$B^{(1.5)} = \frac{1}{\sqrt{\pi}} \begin{bmatrix} 0 & 0 & 0 & 0 \\ 0 & 0 & 0 & 0 \\ 640 & 128 & -\frac{128}{7} & \frac{128}{21} \\ -896 & 640 & \frac{896}{3} & -\frac{640}{11} \end{bmatrix}$$

$$F^{(1.5)} = \frac{1}{\sqrt{\pi}} \begin{bmatrix} 0 & 0 & 0 & 0 \\ 0 & 0 & 0 & 0 \\ 1280 * (1 - \sqrt{2}) & 2^8 * (3\sqrt{2} - 4) & \frac{2^7 * (166 - 118\sqrt{2})}{7} & -\frac{2^8 * (538\sqrt{2} - 824)}{21} \\ 2^8 * (91\sqrt{2} - 28) & -2^8 * (29\sqrt{2} - 51) & -\frac{2^8 * (400 - 281\sqrt{2})}{3} & \frac{2^8 * (10245 - 9557\sqrt{2})}{33} \end{bmatrix}$$

In order to solve the time fractional B-S model of the European option, $U(x, \tau)$ in Equation (9) can be approximated with

$$U(x, \tau) \simeq \Psi(x)^T U \Psi(\tau) \quad (31)$$

where $U = [u_{i,j}]_{M \times M}$ is an unknown matrix, which needs to be determined; from Equation (30), we can obtain

$$\begin{cases} \frac{\partial^\alpha U(x, \tau)}{\partial \tau^\alpha} = \Psi(x)^T U D^\alpha \Psi(\tau) \\ \frac{\partial U(x, \tau)}{\partial x} = \Psi(x)^T D^T U \Psi(\tau) \\ \frac{\partial^2 U(x, \tau)}{\partial x^2} = \Psi(x)^T (D^T)^2 U \Psi(\tau) \end{cases} \quad (32)$$

From Definition 1, Equation (32) can be rewritten as

$$\begin{cases} \frac{\partial^\alpha U(x, \tau)}{\partial \tau^\alpha} = \text{Vec}(\Psi(\tau)^T \otimes \Psi(x)^T) [(D^\alpha)^T \otimes I_M] \text{Vec}(U) \\ \frac{\partial U(x, \tau)}{\partial x} = \text{Vec}(\Psi(\tau)^T \otimes \Psi(x)^T) [I_M \otimes D^T] \text{Vec}(U) \\ \frac{\partial^2 U(x, \tau)}{\partial x^2} = \text{Vec}(\Psi(\tau)^T \otimes \Psi(x)^T) [I_M \otimes (D^T)^2] \text{Vec}(U) \end{cases}$$

where

$$\text{Vec}(\Psi(\tau)^T \otimes \Psi(x)^T) = [\psi_1(\tau)\Psi(x), \psi_2(\tau)\Psi(x), \dots, \psi_M(\tau)\Psi(x)]_{1 \times M^2}$$

and I_M is an M -dimensional identity matrix. Then, Equation (9) can be converted to

$$\begin{cases} \Psi^T(x)UD^\alpha\Psi(\tau) = c_1\Psi(x)^T(D^2)^T U\Psi(\tau) + c_2\Psi(x)^T D^T U\Psi(\tau) + \\ \quad c_3\Psi(x)^T U\Psi(\tau) \\ \Psi^T(x)U\Psi(0) = \Pi(x) \\ \Psi^T(B_d)U\Psi(\tau) = P(\tau) \\ \Psi^T(B_u)U\Psi(\tau) = Q(\tau) \end{cases} \quad (33)$$

Define

$$Z = (D^\alpha)^T \otimes I_M - c_1(I_M \otimes D^T) - c_2[I_M \otimes (D^T)^2] - c_3(I_M \otimes I_M)$$

and let

$$\Delta x = \frac{B_u - B_d}{N_s}, \quad x_i = B_d + i\Delta x, \quad i = 0, 1, 2, \dots, N_s \\ \Delta \tau = T/N_t, \quad \tau_j = j\Delta \tau, \quad j = 0, 1, 2, \dots, N_t$$

be the step size of stock price and time, respectively. Denoting $U_i^j = U(x_i, \tau_j)$ yields

$$\begin{cases} [\text{Vec}(\Psi(x_i)^T \otimes \Psi(\tau_j)^T)Z] \text{Vec}(U) = 0 \\ [\text{Vec}(\Psi(x_i)^T \otimes \Psi(\tau_0)^T)] \text{Vec}(U) = U_i^0 \\ [\text{Vec}(\Psi(x_0)^T \otimes \Psi(\tau_j)^T)] \text{Vec}(U) = U_0^j \\ [\text{Vec}(\Psi(x_{N_s})^T \otimes \Psi(\tau_j)^T)] \text{Vec}(U) = U_{N_s}^j \end{cases} \quad (34)$$

which can be expressed as

$$H\text{Vec}(U) = Y \quad (35)$$

Let

$$L = \begin{bmatrix} \psi_1(x_0) & \psi_2(x_0) & \cdots & \psi_M(x_0) \\ \psi_1(x_1) & \psi_2(x_1) & \cdots & \psi_M(x_1) \\ \vdots & \vdots & \ddots & \vdots \\ \psi_1(x_{N_s}) & \psi_2(x_{N_s}) & \cdots & \psi_M(x_{N_s}) \end{bmatrix}_{(N_s+1) \times M}$$

and

$$K = \begin{bmatrix} \psi_1(\tau_0) & \psi_2(\tau_0) & \cdots & \psi_M(\tau_0) \\ \psi_1(\tau_1) & \psi_2(\tau_1) & \cdots & \psi_M(\tau_1) \\ \vdots & \vdots & \ddots & \vdots \\ \psi_1(\tau_{N_t}) & \psi_2(\tau_{N_t}) & \cdots & \psi_M(\tau_{N_t}) \end{bmatrix}_{(N_t+1) \times M}$$

then

$$H = \begin{bmatrix} (L \otimes K)Z \\ L \otimes K(1,:) \\ L(1,:) \otimes K \\ L(N_s + 1,:) \otimes K \end{bmatrix}$$

and

$$Y = \begin{bmatrix} \underbrace{0, \dots, 0}_{(N_s+1)(N_t+1)}, \underbrace{U_0^0, \dots, U_{N_s}^0}_{N_s+1}, \underbrace{U_0^0, \dots, U_0^{N_t}}_{N_t+1}, \underbrace{U_{N_s}^0, \dots, U_{N_s}^{N_t}}_{N_t+1} \end{bmatrix}$$

5. ELM Algorithm for LWNN Training

ELM has a fast convergence rate owing to its single hidden layer feed-forward structure. It has many advantages over traditional BP methods, because traditional BP methods can easily become stuck in local optima and have a slow convergence rate owing to the continuous weight updating. The parameters of ELM only depend on the analytical resolution of the output layer weights and the random selection of input and hidden layer parameters (weights and biases); as a consequence, many issues, such as the learning rate, local optima and learning epochs, can be avoided. It can solve the slow convergence rate and over-fitting issues of gradient descent methods based on neural networks. Here, the ELM algorithm is illustrated in Algorithm 1. The Neural network structure of LWNN-ELM is showed in Figure 1.

Algorithm 1 Extreme learning machine algorithm.

Input: $A = \{a_i\}_{i=1}^n$, $B = \{b_i\}_{i=1}^n$, $X = \{x_i\}_{i=1}^n$

a_i and b_i denote the weights and bias of the input layer, respectively.

N_i , N_h , N_o represent the nodes of the input, hidden, and output layer, respectively.

Step 1: Attribute random parameters of the hidden layer nodes, weights, and biases.

Step 2: Calculate the output matrix of the hidden layer nodes H .

Step 3: Calculate the output weight $\beta = H^\dagger Y$.

where H^\dagger is the Moore–Penrose generalized inverse of the hidden layer output matrix H , Y is the training data target.

Theorem 4. The equation $H\beta = Y$ can be solved in three cases:

1. If matrix H is square and invertible, then $\beta = H^{-1}Y$.
2. If matrix H is rectangle, then $\beta = H^\dagger Y$; β is the minimal least square solution; in other words, $\beta = \arg \min \|Y\beta - T\|$.
3. If matrix H is singular, then $\beta = H^\dagger Y$, where $H^\dagger = H^T(\lambda I + HH^T)^{-1}$; λ is a regularization parameter, which can be set based on a specific norm.

The procedure for training the network weights of the LWNN to solve the European options pricing model is given in Algorithm 2.

Algorithm 2 The procedure for solving the European options pricing model based on the LWNN-ELM.

Input: $x_i = B_d + i\Delta x$, $\Delta x = (B_u - B_d)/N_s$, $i = 0, 1, 2, \dots, N_s$

$\tau_j = j\Delta\tau$, $\Delta\tau = T/N_t$, $j = 0, 1, 2, \dots, N_t$

$\psi_1(x), \dots, \psi_M(x), \psi_1(\tau), \dots, \psi_M(\tau)$

Step 1: Constructing a numerical solution by the Legendre wavelet as the activation function, that is $U^*(x, \tau) = \sum_{i=0}^n \sum_{j=0}^n \beta_{i,j} \Psi_i(x) \Psi_j(\tau) = \Psi(x, \tau) \beta$.

Step 2: Substituting the numerical solution $U^*(x, \tau)$ and its derivative into the PDEs, the initial condition, and its boundary.

Step 3: Solving $H\beta = Y$ by ELM and obtaining the network weights

$\beta = H^+ Y$, $\beta = \operatorname{argmin} \|H\beta - Y\|$.

Step 4: To obtain the numerical solution

$U^*(x, \tau) = \sum_{i=0}^n \sum_{j=0}^n \beta_{i,j} \Psi_i(x) \Psi_j(\tau) = \Psi(x, \tau) \beta$.

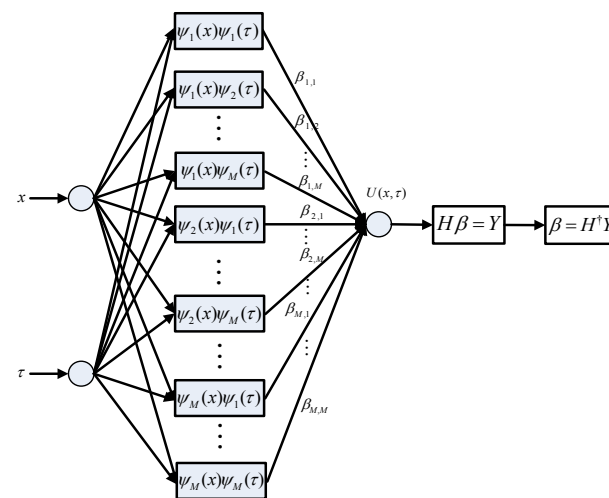


Figure 1. Neural network structure based on the LWNN-ELM, where x and τ denote the stock price and time, respectively.

Remark 2. The detailed proof of this theorem can be referred to the related knowledge of the generalized inverse matrix [43].

6. Numerical Experiment and Discussion

Once the numerical solution is obtained for a specific options pricing model, the main concern of market practitioners becomes its implementation. Whether the options price can be efficiently computed is one of the core criteria to evaluate its characteristics. Therefore, in this section, as far as the validation of the numerical solution's accuracy and the convergence order of the proposed method are concerned, a double barrier knock-out call European option is selected as an experiment. For other kinds of options pricing models, their solutions can be straightforwardly obtained by a simple modification or the parity relationship [75].

In order to validate the feasibility of the proposed method, calculating the solution for $\alpha = 1$ can be considered as the best way, and comparing it with a benchmark solution based on the implicit difference method (IDM) [22], where all numerical experiments were implemented with MATLAB R2013b on a desktop with i7-6700K CPU, 8GB memory, 1TB HDD, and a Windows 7 operating system. From Figure 2, it can be seen that the two groups of options price coincide perfectly, which can affirm the correctness of the proposed method. Besides, the calculation times for different expirations is presented in Table 1; it is clear that the time consumption of the LWNN-ELM method decreases significantly compared with the IDM, which can save computing resources.

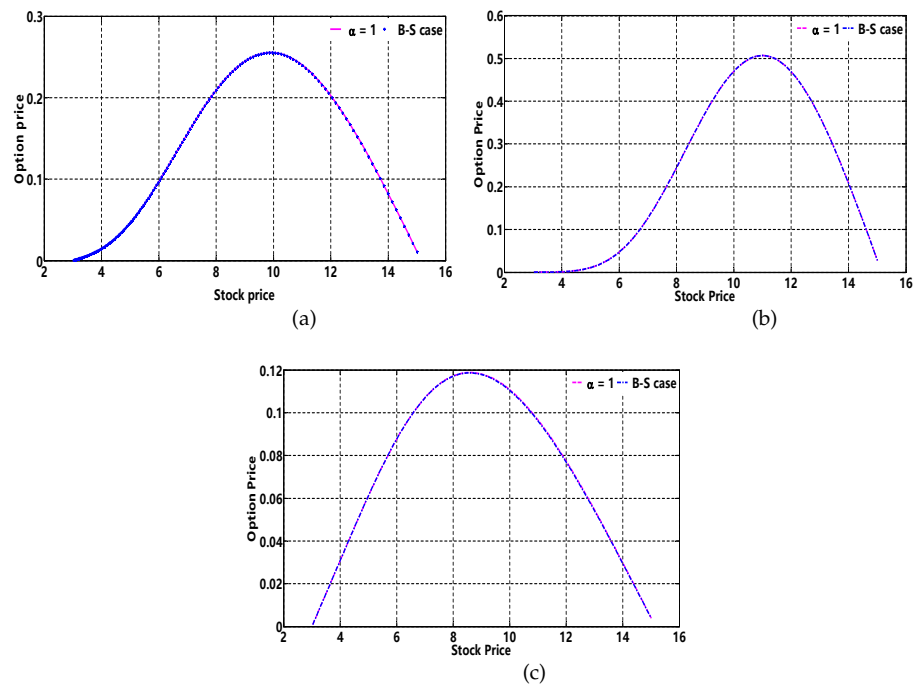


Figure 2. Comparison of the solution at $\alpha = 1$ with the traditional B-S model, where the corresponding parameters are $\sigma = 0.45$, $r = 0.03$, $q = 0.01$, $K = 10$, $A = 3$, $B = 15$, and $M = 16$. (a) $T = 1$ (years); (b) $T = 0.5$; (c) $T = 2$.

Table 1. Time consumption of the LWNN-ELM and IDM for different expirations.

Time Consumption (seconds)	Method	LWNN-ELM	IDM
Expiration (years)			
1		5.2853	75.2167
0.5		4.3862	62.4791
2		6.7541	83.3754

Here, the influence of different α on the options price is investigated. From Equation (6), intuitively, α can be regarded as a metric of the dependence of $U(S, t)$ on the stock price at the same underlying level from the current time to the expiration; in the practical case, $T - t \leq 1$; it is not difficult to observe that the larger α is, the weaker the dependence becomes. This may explain the phenomena illustrated in Figure 3, wherein the B-S model tends to overprice a double knock-out call when the underlying is close to the lower barrier. On the other hand, it can be observed that from a certain underlying value and onward, this B-S model prefers to underprice the option, which possibly results in the larger impact of the nonzero payoff value on the options price for smaller α . Table 2 offers the calculation time of the LWNN-ELM for different expirations; it can be seen that for a longer expiration, the time consumption has no apparent increase which is beneficial for some complex options pricing models.

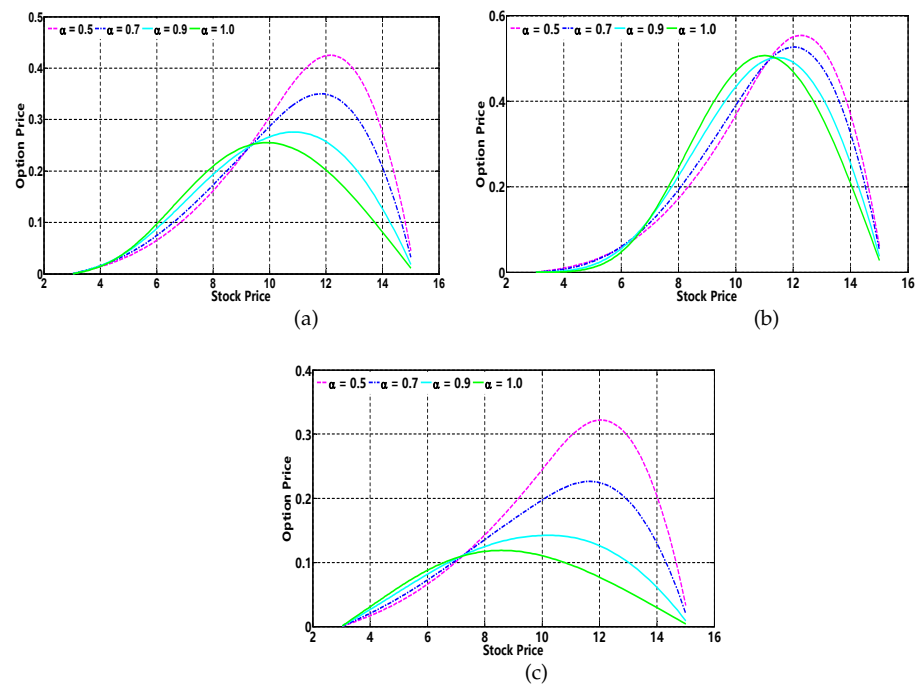


Figure 3. Options price for different α , where the corresponding parameters are $\sigma = 0.45$, $r = 0.03$, $q = 0.01$, $K = 10$, $A = 3$, $B = 15$, and $M = 16$. (a) $T = 1$ (years); (b) $T = 0.5$; (c) $T = 2$.

Table 2. Time consumption of the LWNN-ELM for different expirations.

Time Consumption (seconds)	Method
Expiration (years)	LWNN-ELM
1	27.6381
0.5	24.9635
2	31.7652

For the European put option, the final and boundary conditions are $\bar{\Pi}(S) = \max\{K - S, 0\}$, $\bar{Q}(t) = q = 0$, and $\bar{P}(t) = K \exp(-r(T - t))$. The put options prices for different M are presented in Figure 4; it is clear that the numerical solutions of the LWNN-ELM for different M are quite close; meanwhile, the time consumption is 4.8391 ($M = 12$) and 6.1726 ($M = 16$), respectively. In addition, the numerical solutions based on the LWNN-ELM and IDM are provided in Table 3; it is clear that the numerical solutions obtained by the LWNN-ELM agree very well with the benchmark method. Although the numerical solution for $M = 12$ has a faster computation rate compared to that of $M = 16$, the numerical solution for $M = 16$ has a higher precision. Consequently, for a more accurate description of financial dynamics, a fast and efficient scheme to solve the options price is preferred. In the end, the order of convergence is utilized to explore the solution accuracy [76], which is defined as

$$\text{Order} = \log_2 \frac{\|e_{\Delta\tau}\|_{\infty}}{\|e_{(\Delta\tau/2)}\|_{\infty}} \quad (36)$$

where $e_{(\Delta\tau)} = U_{(\Delta\tau)} - U_{(\Delta\tau/2)}$ and $U_{(\Delta\tau)}$ is the numerical solution at the final time with step size $\Delta\tau$. In the following experiments, $N_s = 460$ was selected to saturate the stock price discretization so that the error is mainly determined by the time discretization. The order of convergence of the European option is illustrated in Table 4. It can be observed that the LWNN-ELM has first-order convergence for different α .

Table 3. The numerical solutions of the European put option, where the corresponding parameters are $K = 50$, $T = 1$, $r = 0.01$, $\sigma = 0.1$, $A = 10$, $B = 100$, and $M = 16$.

(N_s, N_t)	Method	Stock Price					
		$S = 30$	$S = 40$	$S = 50$	$S = 60$	$S = 70$	$S = 80$
(230,500)	LWNN-ELM	17.6089	9.0658	3.5568	1.1969	0.4472	0.1727
	IDM	17.6088	9.0656	3.5571	1.1968	0.4473	0.1726
(460,500)	LWNN-ELM	17.5861	9.2083	3.5714	1.2866	0.4707	0.1757
	IDM	17.5862	9.2083	3.5715	1.2867	0.4706	0.1755

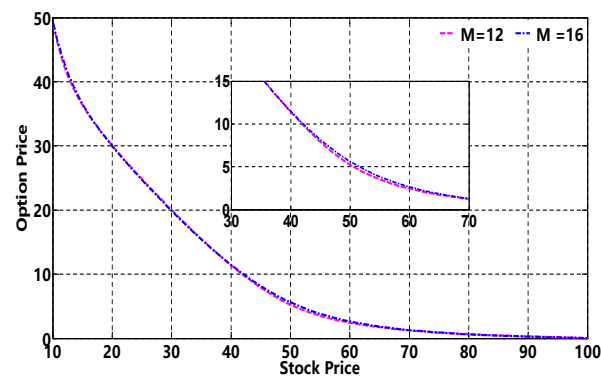


Figure 4. European put options price obtained by the LWNN-ELM for different M , where the corresponding parameters are $\alpha = 0.7$, $K = 50$, $T = 1$, $r = 0.01$, $\sigma = 0.1$, $A = 10$, and $B = 100$.

Table 4. The convergence order of the European put options price. N_t is the number of discretization points regarding time; the number of discretization points regarding the stock price is fixed as $N_s = 460$.

$\alpha \backslash N_t$	0.1	0.2	0.3	0.4	0.5	0.6	0.7	0.8	0.9
250	1.02	1.05	1.02	1.04	1.02	1.04	1.02	1.02	0.98
500	1.01	1.01	1.03	1.03	1.01	1.00	1.04	0.99	1.01
1000	1.01	1.01	1.00	1.02	1.00	1.03	1.02	1.02	0.99
2000	1.00	1.00	1.02	1.01	1.01	1.00	0.99	1.01	0.99

7. Conclusions

Being a generalization of the classic B-S model, the “global” characteristic of the time fractional B-S model makes it more difficult to calculate the analytical or numerical solution than the integer-order model. In this paper, the options price model is governed by a time fractional derivative B-S equation when the underlying price change is considered as a fractal transmission system, then the fractional derivative operational matrix of the two-dimensional Legendre wavelet is derived, and the European options pricing model (including final and boundary conditions) is transformed to a group of algebraic equations. The LWNN-ELM is employed to train the output layer weights owing to its fast learning rate and moderate fitting characteristic. In the end, numerical experiments are provided to price the European option with double barriers based on the LWNN-ELM and the implicit differential method, and the experimental results illustrate that the proposed method has less time consumption compared with the benchmark method; besides, the first-order convergence is demonstrated when α is less than 1. Furthermore, the proposed scheme is simple and easy to implement and can be available to other similar fractional models for pricing different European options.

Author Contributions: Conceptualization, X.Z. and Y.Z.; methodology, X.Z.; software, Y.Z.; validation, J.Y. and Y.Z.; formal analysis, X.Z.; investigation, X.Z. and Y.Z.; resources, X.Z.; data curation, Y.Z.; writing—original draft preparation, X.Z. and Y.Z.; writing—review and editing, X.Z.; visualization, Y.Z.; supervision, J.Y.; project administration, J.Y.; funding acquisition, J.Y. All authors have read and agreed to the published version of the manuscript.

Funding: This research was funded by the National Natural Science Foundation of China under Grant No. U1901223 and the Natural Science Foundation of Guangdong Province under Grant No. 2014B080807027.

Institutional Review Board Statement: The study was approved by the Academic Committee of South China University of Technology.

Informed Consent Statement: Not applicable.

Data Availability Statement: No data were used to support this study.

Acknowledgments: The authors thank all of the Reviewers for their valuable suggestions and recommendation, which contributed to this manuscript's improvement.

Conflicts of Interest: The authors declare no conflict of interest.

Abbreviations

The following abbreviations are used in this manuscript:

B-S	Black–Scholes
ELM	Extreme learning machine
LWNN	Legendre wavelet neural network
PDE	Partial differential equation
WNN	Wavelet neural network
BP	Back-propagation
CPU	Central processing unit
HDD	Hard disk drive

References

- Podisuk, M. Regulatory quality, financial integration and equity cost of capital. *Rev. Int. Econ.* **2019**, *27*, 916–935.
- Clère, R. A new way to estimate cost of capital. *J. Int. Fin. Manag. Acc.* **2019**, *4*, 223–249. [\[CrossRef\]](#)
- Basu, P. Capital adjustment cost and inconsistency in inconsistency dynamic panel models with fixed effects. *Ger. Econ. Rev.* **2019**, *20*, 1002–1018. [\[CrossRef\]](#)
- Staveley-O'Carroll, J. Exchange rate targeting in the presence of foreign debt obligations. *J. Macroecon.* **2018**, *56*, 113–134. [\[CrossRef\]](#)
- Dudin, B. Resource Allocation with Automated QoE Assessment in 5G/B5G Wireless Systems. *IEEE Netw.* **2019**, *33*, 76–81. [\[CrossRef\]](#)
- Dudin, B. OKRA: Optimal task and resource allocation for energy minimization in mobile edge computing systems. *Wirel. Netw.* **2019**, *25*, 2851–2867.
- Samuelson, P.A.; Davis, M.; Etheridge, A. *Louis Bachelier's Theory of Speculation: The Origins of Modern Finance*; Princeton University Press: Princeton, NJ, USA, 2006.
- Black, F. The pricing of options and corporate liabilities. *J. Polit. Econ.* **1973**, *81*, 637–654. [\[CrossRef\]](#)
- Merton, R.C. Theory of rational options pricing. *J. Econ. Manag. Sci.* **1973**, *4*, 141–183. [\[CrossRef\]](#)
- Wu, C.L. The Finite Moment Log Stable Process and Option Pricing. *J. Financ.* **2003**, *58*, 753–777.
- Fallahgoul, H.A.; Focardi, S.M.; Fabozzi, F.J. *Fractional Calculus and Fractional Processes with Applications to Financial Economics*; Academic Press: London, UK, 2016.
- Caputo, M. Linear Models of Dissipation whose Q is almost Frequency Independent—II. *Geophys. J. Int.* **1966**, *19*, 529–539. [\[CrossRef\]](#)
- Caputo, M. Modified Riemann–Liouville derivative and fractional Taylor series of nondifferentiable functions further results. *Comput. Math. Appl.* **2006**, *51*, 1367–1376.
- Guariglia, E.; Silvestrov, S. Fractional-wavelet analysis of positive definite distributions and wavelets on $\mathcal{D}'(\mathbb{C})$. In *Engineering Mathematics II*; Springer: Berlin/Heidelberg, Germany, 2016; pp. 337–353.
- Berry, M.V.; Lewis, Z.V. On the Weierstrass-Mandelbrot Fractal Function. *Proc. Soc. Lond.* **1980**, *370*, 459–484.
- Lin, Y.; Xu, C. Implicit finite difference approximation for time fractional diffusion equations. *Comput. Math. Appl.* **2008**, *56*, 1138–1145.

17. Langlands, T.A.M.; Henry, B.I. The accuracy and stability of an implicit solution method for the fractional diffusion equation. *J. Comput. Phys.* **2005**, *205*, 719–736. [\[CrossRef\]](#)
18. Chen, W.; Xiang, X.; Zhu, S.P. Analytically pricing European-style options under the modified Black–Scholes equation with a spatial-fractional derivative. *Q. Appl. Math.* **2014**, *72*, 597–611. [\[CrossRef\]](#)
19. Song, L.; Wei, G. Solution of the Fractional Black–Scholes Option Pricing Model by Finite Difference Method. *Abstract Appl. Anal.* **2013**, *6*, 1–16. [\[CrossRef\]](#)
20. Cen, Z.; Huang, J.; Xu, A.; Le, A. Numerical approximation of a time-fractional Black–Scholes equation. *Comput. Math. Appl.* **2018**, *75*, 2874–2887. [\[CrossRef\]](#)
21. Rezaei, M.; Yazdani, A.R.; Ashrafi, A.; Mahmoudi, S.M. Numerical pricing based on fractional Black–Scholes equation with time-dependent parameters under the CEV model: Double barrier options. *Comput. Math. Appl.* **2021**, *90*, 104–111. [\[CrossRef\]](#)
22. Zhang, H.; Liu, F.; Turner, I.; Yang, Q. Numerical solution of the time fractional Black–Scholes model governing European options. *Comput. Math. Appl.* **2016**, *71*, 1772–1783. [\[CrossRef\]](#)
23. Staelen, R.H.; Hendy, A.S. Numerically pricing double barrier options in a time-fractional Black–Scholes model. *Comput. Math. Appl.* **2017**, *74*, 1166–1175. [\[CrossRef\]](#)
24. Yavuz, M.; Özdemir, N. A different approach to the European options pricing model with new fractional operator. *Math. Model. Nat. Phenom.* **2018**, *13*, 1–13. [\[CrossRef\]](#)
25. Yavuz, M.; Özdemir, N. European vanilla options pricing model of fractional order without singular kernel. *Fractal Fract.* **2018**, *2*, 1–12. [\[CrossRef\]](#)
26. Elbeleze, A. A.; Kilicman, A.; Taib, B. M. Homotopy Perturbation Method for Fractional Black–Scholes European Option Pricing Equations Using Sumudu Transform. *Math. Probl. Eng.* **2013**, 2013, 1–7. [\[CrossRef\]](#)
27. Kumar, S.; Kumar, D.; Singh, J. Numerical computation of fractional Black–Scholes equation arising in financial market. *Egypt. J. Basic Appl. Sci.* **2014**, *1*, 177–183. [\[CrossRef\]](#)
28. Park, S.H.; Kim, J.H. Homotopy analysis method for options pricing under stochastic volatility. *Appl. Math. Lett.* **2011**, *24*, 1740–1744. [\[CrossRef\]](#)
29. Gülka, V. The homotopy perturbation method for the Black–Scholes equation. *J. Stat. Comput. Simul.* **2010**, *80*, 1349–1354. [\[CrossRef\]](#)
30. Liao, S. *Homotopy Analysis Method in Nonlinear Differential Equations*; Higher Education Press: Beijing, China, 2012.
31. Ahmad, J.; Shakeel, M.; Hassan, Q.; Mahmood, U.; Mohyud-Din, S.T. Analytical solution of Black–Scholes model using fractional variational iteration method. *Int. J. Mod. Math. Sci.* **2013**, *5*, 133–142.
32. Baleanu, D.; Srivastava, H. M.; Yang, X.J. Local fractional variational iteration algorithms for the parabolic Fokker–Planck equation defined on Cantor sets. *Prog. Fract. Differ. Appl.* **2015**, *1*, 1–10.
33. Yavuz, M.; Ozdemir, N.; Okur, Y.Y. Generalized differential transform method for fractional partial differential equation from finance. In Proceedings of the International Conference on Fractional Differentiation and its Applications, Novi Sad, Serbia, 18–20 July 2016.
34. Yavuz, M.; Zdemir, N. A Quantitative Approach to Fractional Option Pricing Problems with Decomposition Series. *Appl. Math. Sci.* **2018**, *6*, 102–109.
35. Edeki, S.O.; Motsepa, T.; Khalique, C.M. The Greek parameters of a continuous arithmetic Asian options pricing model via Laplace Adomian decomposition method. *Open Phys.* **2018**, *16*, 780–785. [\[CrossRef\]](#)
36. Daftardar-Gejji, V.; Jafari, H. Adomian decomposition: a tool for solving a system of fractional differential equations. *J. Math. Anal. Appl.* **2015**, *301*, 508–518. [\[CrossRef\]](#)
37. El-Borai, M.M.; El-Sayed, W.G.; Jawad, A.M. Adomian Decomposition Method For solving Fractional Differential Equations. *Int. Res. J. Eng. Technol.* **2015**, *2*, 296–306.
38. Wyss, W. The fractional Black–Scholes equation. *Fract. Calc. Appl. Anal.* **2000**, *3*, 51–61.
39. Hu, Y.; OKsendal, B. Fractional White Noise Calculus and Applications to Finance. *Infin. Dimens. Anal. Quantum Probab. Relat. Top.* **2003**, *6*, 1–32. [\[CrossRef\]](#)
40. Li, Q.; Zhou, Y.; Zhao, X.; Ge, X. Fractional Order Stochastic Differential Equation with Application in European Option Pricing. *Discrete Dyn. Nat. Soc.* **2014**, 2014, 1–12. [\[CrossRef\]](#)
41. Jumarie, G. Derivation and solutions of some fractional Black–Scholes equations in coarse-grained space and time. Application to Merton’s optimal portfolio. *Comput. Math. Appl.* **2010**, *59*, 1142–1164. [\[CrossRef\]](#)
42. Liu, H. K.; Chang, J.J. A closed-form approximation for the fractional Black–Scholes model with transaction costs. *Comput. Math. Appl.* **2013**, *56*, 1719–1726. [\[CrossRef\]](#)
43. Huang, G.B.; Zhu, Q.Y.; Siew, C.K. Extreme learning machine: theory and applications. *Neural Comput.* **2006**, *70*, 489–501. [\[CrossRef\]](#)
44. Albadra, M.A.A.; Tiuna, S. Extreme Learning Machine: A Review. *Int. J. Appl. Eng. Res.* **2017**, *12*, 4610–4623.
45. Li, C.; Xue, D.; Hu, Z.; Chen, H. A Survey for Breast Histopathology Image Analysis Using Classical and Deep Neural Networks. In *International Conference on Information Technologies in Biomedicine*; Springer: Berlin/Heidelberg, Germany, 2019.
46. Wang, J.; Chen, Y.; Hao, S.; Peng, X.; Hu, L. Deep Learning for Sensor-based Activity Recognition: A Survey. *Pattern Recognit. Lett.* **2017**, *119*, 3–11. [\[CrossRef\]](#)

47. Bahiuddin, I.; Mazlan, S.A.; Shapiai, M.I. Study of extreme learning machine activation functions for magnetorheological fluid modelling in medical devices application. In Proceedings of the International Conference on Robotics, Automation and Sciences, Nelaka, Malaysia, 27–29 November 2017.
48. Liu, X.; Lin, S.; Fang, J.; Xu, Z. Is extreme learning machine feasible? A theoretical assessment (part I). *IEEE Trans. Neural Netw. Learn. Syst.* **2015**, *26*, 7–20. [[CrossRef](#)] [[PubMed](#)]
49. Lin, S.; Liu, X.; Fang, J.; Xu, Z. Is Extreme Learning Machine Feasible? A Theoretical Assessment (Part II). *IEEE Trans. Neural Netw. Learn. Syst.* **2017**, *26*, 21–34. [[CrossRef](#)] [[PubMed](#)]
50. Venkatesh, S.G.; Ayyaswamy, S.K.; Balachandar, S.R. The Legendre wavelet method for solving initial value problems of Bratu-type. *Comput. Math. Appl.* **2012**, *63*, 1287–1295. [[CrossRef](#)]
51. Heydari, M.H.; Hooshmandasl, M.R.; Ghaini, F. A new approach of the Chebyshev wavelets method partial differential equations with boundary conditions of the telegraph type. *Appl. Math. Model.* **2014**, *38*, 1597–1606. [[CrossRef](#)]
52. Keshavarz, E.; Ordokhani, Y.; Razzaghi, M. The Taylor wavelets method for solving the initial and boundary value problems of Bratu-type equations. *Appl. Numer. Math.* **2018**, *128*, 205–216. [[CrossRef](#)]
53. Zheng, X.; Tang, Y.Y.; Zhou, J. A framework of adaptive multiscale wavelet decomposition for signals on undirected graphs. *IEEE Trans. Signal Process.* **2019**, *67*, 1696–1711. [[CrossRef](#)]
54. Zhang, Q. and Benveniste, A. Wavelet network. *IEEE Trans. Neural Netw.* **1992**, *3*, 889–898. [[CrossRef](#)]
55. Zhang J.; Walter, G.G.; Miao, Y.; Wavelet neural networks for function learning. *IEEE Trans. Signal Process.* **1995**, *43*, 1485–1497. [[CrossRef](#)]
56. Daugman, J.G. Complete discrete 2-D Gabor transforms by neural networks for image analysis and compression. *IEEE Trans. Audio Speech Lang. Process.* **1988**, *36*, 1169–1179. [[CrossRef](#)]
57. Hussain, A.J.; Al-Jumeily, D.; Radi, N.; Lisboa, P. Hybrid Neural Network Predictive-Wavelet Image Compression System. *Neurocomputing* **2015**, *151*, 975–984. [[CrossRef](#)]
58. Shi, J.; Zhao, Y.; Xiang, W. Deep Scattering Network with Fractional Wavelet Transform. *IEEE Trans. Signal Process.* **2021**, *69*, 4740–4757. [[CrossRef](#)]
59. Shi, J.; Liu, X.; Xiang, W. Novel fractional wavelet packet transform: theory, implementation, and applications. *IEEE Trans. Signal Process.* **2020**, *68*, 4041–4054. [[CrossRef](#)]
60. Jahangiri, F.; Doustmohammadi, A.; Menhaj, M.B. An adaptive wavelet differential neural networks based identifier and its stability analysis. *Neurocomputing* **2012**, *77*, 12–19. [[CrossRef](#)]
61. Pan, H.; Xia, L.Z. Efficient Object Recognition Using Boundary Representation and Wavelet Neural Network. *IEEE Trans. Neural Netw.* **2008**, *19*, 2132–2148. [[CrossRef](#)]
62. Liang, J.R.; Wang, J.; Zhang, W.J.; Qiu, W.Y.; Ren, F.Y. The solutions to a bi-fractional black-scholes-merton differential equation. *Int. J. Pure Appl. Math* **2010**, *128*, 99–112.
63. Giona, M.; Roman, H.E. Fractional diffusion equation on fractals: One-dimensional case and asymptotic behaviour. *J. Phys. A-Math. Gen.* **1999**, *25*, 2093. [[CrossRef](#)]
64. Mehaute, A.L. Transfer processes in fractal media. *J. Phys. A-Math. Gen.* **1984**, *36*, 665–676. [[CrossRef](#)]
65. Jumarie, G. Stock exchange fractional dynamics defined as fractional exponential growth driven by (usual) Gaussian white noise. Application to fractional Black–Scholes equations. *Insur. Math. Econ.* **2008**, *42*, 271–287. [[CrossRef](#)]
66. Jumarie, G. Merton’s model of optimal portfolio in a Black–Scholes Market driven by a fractional Brownian motion with short-range dependence. *Insur. Math. Econ.* **2005**, *37*, 585–598. [[CrossRef](#)]
67. Hussaini, M.Y.; Zang, T.A. *Spectral Methods in Fluid Dynamics*; Springer: Berlin, Germany, 1986.
68. Razzaghi, M.; Yousefi, S. Legendre wavelets direct method for variational problems. *Math. Comput. Simul.* **2000**, *63*, 185–192. [[CrossRef](#)]
69. Kreyszig, E. *Introduction Functional Analysis with Applications*; Wiley: New York, NY, USA, 1978.
70. Liu, N.; Lin, E.B. Legendre wavelet method for numerical solutions of partial differential equations. *Numer. Meth. Part Differ. Equ.* **2010**, *26*, 81–94. [[CrossRef](#)]
71. Heydari, M.H.; Hooshmandasl, M.R.; Ghaini, F.M. M. Two-dimensional Legendre wavelets for solving fractional Poisson equation with Dirichlet boundary conditions. *Eng. Anal. Bound. Elem.*, **2013** *37*, 1331–1338. [[CrossRef](#)]
72. Steeb, W.H.; Shi, T.K. *Matrix Calculus and Kronecker Product with Applications and C++ Programs*; World Scientific Publishing Company: Singapore, 1997.
73. Hardy, Y.; Steeb, W. *Problems and Solutions in Introductory and Advanced Matrix Calculus*; World Scientific Publishing Company: Singapore, 2016.
74. Podlubny, I. Fractional Differential Equations. In *Mathematics in Science and Engineering*; Academic Press: San Diego, CA, USA, 1999.
75. Faulhaber, O. Analytic Methods for Pricing Double Barrier Options in the Presence of Stochastic Volatility. Ph.D. Thesis, Technische Universitat Kaiserslautern, Kaiserslautern, Germany, 2002.
76. Chen, C.; Wang, Z.; Yang, Y. A new operator splitting method for American options under fractional Black–Scholes models. *Comput. Math. Appl.* **2019**, *77*, 2130–2144. [[CrossRef](#)]